analytical chemistry

pubs.acs.org/ac Article

Rational Design and Development of SARS-CoV-2 Serological Diagnostics by Immunoprecipitation-Targeted Proteomics

Zhiqiang Fu,[§] Yasmine Rais,[§] Delaram Dara, Dana Jackson, and Andrei P. Drabovich*

Cite This: *Anal. Chem.* 2022, 94, 12990−12999 Read Online

ACCESS | Metrics & More | Article Recommendations | Supporting Information

ABSTRACT: Current design of serological tests utilizes conservative immunoassay approaches and is focused on fast and convenient assay development, throughput, straightforward measurements, and affordability. Limitations of common serological assays include semiquantitative measurements, cross-reactivity, lack of reference standards, and no differentiation between human immunoglobulin subclasses. In this study, we suggested that a combination of immunoaffinity enrichments with targeted proteomics would enable rational design and development of serological assays of infectious diseases, such as COVID-19. Immunoprecipitation-targeted proteomic assays allowed for sensitive and specific measurements of NCAP_SARS2 protein with a limit of detection of 313 pg/mL in serum and enabled differential quantification of anti-SARS-CoV-2 antibody isotypes (IgG, IgA, IgM, IgD, and IgE) and individual subclasses (IgG1-4 and IgA1-2) in plasma and saliva. Simultaneous evaluation of the numerous antigen−antibody subclass combinations revealed a receptor-binding domain (RBD)-IgG1 as a combination with the highest diagnostic performance. Further validation revealed that anti-RBD IgG1, IgG3, IgM, and IgA1 levels were significantly elevated in convalescent plasma, while IgG2, IgG4, and IgA2 were not informative. Anti-RBD IgG1 levels in convalescent (2138 ng/mL) vs negative (95 ng/mL) plasma revealed 385 ng/mL as a cutoff to detect COVID-19 convalescent plasma. Immunoprecipitation-targeted proteomic assays will facilitate improvement and standardization of the existing serological tests, enable rational design of novel tests, and offer tools for the comprehensive investigation of immunoglobulin subclass cooperation in immune response.

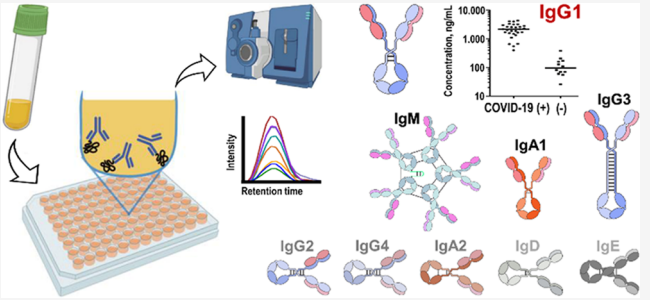

INTRODUCTION

Conventional diagnostics of viral infections relies on the detection of viral genomes by polymerase chain reaction (PCR) or RT-PCR, with the recognized limitations of RNA degradation,[1] relatively high false negative rates,[2] and lack of prognostic information.[3] Alternative assays for diagnostics of viral infections include serological tests to detect circulating antiviral immunoglobulins or protein antigens in blood and proximal fluids. Serological tests enable the detection of past infections, evaluate immune status, and provide prognostic information.[4] Recently, combined tests to measure circulating antiviral immunoglobulins and protein antigens were developed to complement RT-PCR diagnostics and facilitate earlier detection of viral infections.[5]

Enzyme-linked immunosorbent assay (ELISA) and lateral flow immunoassays, the conventional tools for serological diagnostics, present highly sensitive, robust, and convenient assays to measure antiviral immunoglobulins in blood or proximal fluids.[6] Limitations of indirect immunoassays, however, include semiquantitative measurements, lack of international reference standards, challenges with multiplexing, and potential cross-reactivity.[4] Cross-reactivity results in lower diagnostic specificity and prohibits screening of the general asymptomatic population for the acquired immunity against low-prevalence diseases.[7] Redesign of serological tests may minimize cross-reactivity and facilitate the development of tests with higher diagnostic specificity. To ensure simplicity and convenience, common serological tests do not resolve between individual immunoglobulin isotypes (total IgG, total IgA, IgM, IgD, and IgE) and subclasses (IgG1-4, IgA1-2), even though assessment of the complete isotype- and subclass-specific humoral immune response could provide complimentary diagnostic and prognostic information.

Mass spectrometry (MS) with its near-absolute analytical selectivity and multiplexing capabilities presents an alternative approach for serological assays.[8] MS has recently been used for the identification and quantification of SARS-CoV-2 proteins in biological and clinical samples.[9−13] However, without extensive fractionation to reduce sample complexity, MS

Received: March 25, 2022
Accepted: August 31, 2022
Published: September 12, 2022

https://doi.org/10.1021/acs.analchem.2c01325
Anal. Chem. 2022, 94, 12990−12999

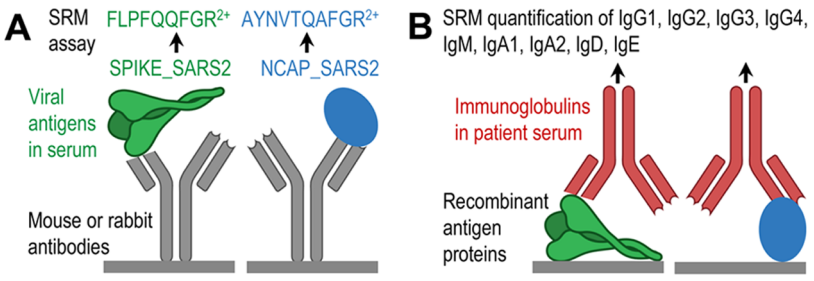

Figure 1. Setup of serological assays by immunoprecipitation-targeted proteomics. IP-SRM or IP-PRM assays for the quantification of SPIKE_SARS2 and NCAP_SARS2 proteins (A) and human immunoglobulin isotypes (IgG, IgM, IgA, IgD, and IgE) and subclasses IgG1-4 and IgA1-2 (B).

assays presented relatively poor analytical and diagnostics sensitivities.

In this study, we hypothesized that a combination of immunoaffinity enrichments with MS measurements could resolve some critical limitations of serological assays. We suggested that immunoprecipitation (IP) combined with selected reaction monitoring (SRM) or parallel reaction monitoring (PRM) targeted proteomic assays could facilitate sensitive and selective quantification of SARS-CoV-2 protein antigens and anti-SARS-CoV-2 immunoglobulins in blood serum or plasma. The proposed IP-SRM or IP-PRM assays (Figure 1) would provide a single platform for: (i) quantification of SARS-CoV-2 proteins in biological samples; (ii) differential quantification of anti-SARS-CoV-2 immunoglobulin isotypes (IgG, IgA, IgM, IgD, and IgE) and subclasses (IgG1-4, IgA1-2); (iii) rational design of serological diagnostics through the selection of antigen−immunoglobulin subclass combinations with the highest diagnostic performance; and (iv) standardization of antigen and immunoglobulin assays via stable, pure, and affordable synthetic peptide internal standards.

EXPERIMENTAL SECTION

Additional details on the methods and reagents can be found in the Supporting Information.

Clinical Specimens. Negative and COVID-19 convalescent plasma, serum, and saliva samples were obtained from the Canadian Biosample Repository and Innovative Research (Table S1). Patient inclusion and exclusion criteria are presented in the Supporting Information. The study was approved by the University of Alberta (#Pro00104098).

Proteins, Antibodies, and Peptide Standards. Antibodies, recombinant NCAP_SARS2 nucleoprotein (N), and SPIKE_SARS2 spike glycoprotein domains S-ECD (extracellular domain), S1 (S1 subunit), and RBD (receptor-binding domain) were obtained from Sino Biological (Table S2). Synthetic stable isotope-labeled peptides standards were provided by JPT Peptide Technologies.

Immunoprecipitation. High-binding microplates were coated with anti-NCAP_SARS2 or anti-SPIKE_SARS2 antibodies (0.5 μg/well), incubated overnight, blocked with 2% bovine serum albumin (BSA), and washed. Human serum (50 μL) was spiked with recombinant proteins, diluted with 0.1% BSA, incubated for 2 h, and washed with 50 mM ammonium bicarbonate. To measure human immunoglobulins, microplates were coated overnight with recombinant S-ECD, S1, RBD, or N proteins (0.5 μg/well), blocked with 2% BSA, and washed. NanoLC-SRM assays required 4 μL of serum (diluted to 100 μL/well), while IP-HPLC-SRM assays required 20 μL of serum or plasma or 33 μL of saliva per patient.

Proteomic Sample Preparation. Following 2 h on-plate incubation and washing, enriched proteins or immunoglobulins were reduced with dithiothreitol, alkylated with iodoacetamide, and digested on the same plate with trypsin (0.25 μg/well). SpikeTides_TQL (Table S3) and SpikeTides_L (Table S4) peptide internal standards (100 fmol/well) were spiked either before or after reduction, alkylation, and digestion, respectively. Tryptic peptides were concentrated with C18 microextraction.

LC-Shotgun MS/MS. Best proteotypic peptides were identified by shotgun liquid chromatography-tandem mass spectrometry (LC-MS/MS) using Orbitrap Elite mass spectrometer with nanoelectrospray ionization source coupled to EASY-nLC II nanoLC (Thermo Scientific). Profile MS1 scans (400−1250 m/z; 60 K resolution) were followed by top 20 ion trap MS/MS scans. Raw files were searched with MaxQuant v1.6.3.4 and NCBI Reference Sequences of SARS-CoV-2 proteins. Modifications included constant cysteine carbamidomethylation and variable methionine oxidation, N-terminal acetylation, and asparagine deamidation. Raw MS data are publicly available.[14]

Development of SRM and PRM Assays. Proteotypic peptides with the highest intensities were selected, synthesized as SpikeTides_L peptides, and used for SRM/PRM assay development. Absolute quantification of S-ECD and N proteins was completed with SpikeTides_TQL peptides. Peptide Atlas, proteinBLAST, neXtProt, and gnomAD databases confirmed the uniqueness of proteotypic peptides and excluded post-translational modifications, allotype variants, and high-frequency single amino acid variants (Table S4). Heavy and light peptides were initially monitored with unscheduled SRM assays (10 transitions per precursor; 5 ms). Low-intensity and high-interference transitions were removed, and three transitions per precursor were scheduled (Tables S5 and S6). Raw MS files were analyzed with Skyline (v20.1.0.76). The peak boundaries were adjusted manually, and L/H peak area ratios were used for the accurate relative or absolute quantification of SARS-CoV-2 proteins or human immunoglobulins. Skyline and raw MS files were deposited to Peptide Atlas (identifier PASS01745 and password JP6573p; www.peptideatlas.org/PASS/PASS01745 or ftp://PASS01745:JP6573p@ftp.peptideatlas.org).

NanoLC-PRM and SRM Assays. Q Exactive coupled to EASY-Spray source and EASY-nLC 1000 nanoLC (Thermo Scientific) were utilized for PRM assays. QTRAP 5500, NanoSpray III source (SCIEX), and EASY-nLC II were used for SRM assays. Peptides were loaded at 5 μL/min onto pre-

https://doi.org/10.1021/acs.analchem.2c01325
Anal. Chem. 2022, 94, 12990−12999

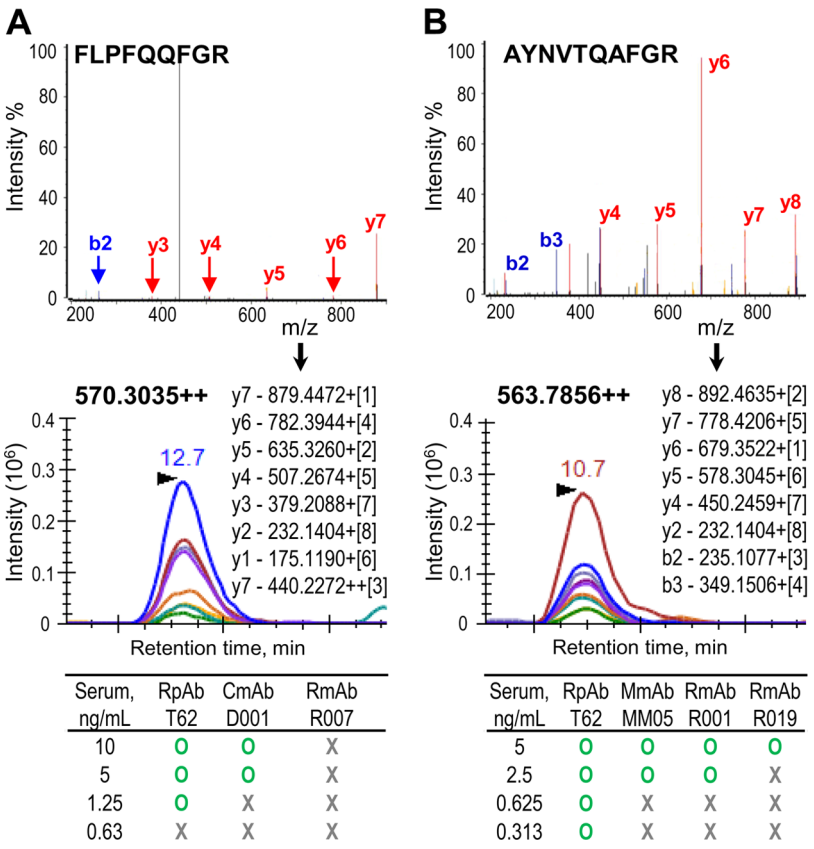

Figure 2. Development of IP-PRM assays for quantification of SPIKE_SARS2 and NCAP_SARS2 proteins. Shotgun LC-MS/MS facilitated the selection of proteotypic peptides and transitions. (A) SPIKE_SARS2 immunoprecipitation-PRM assays were developed with anti-SPIKE_SARS2 chimeric monoclonal CmAb (D001), rabbit monoclonal RmAb (R007), and rabbit polyclonal RpAb (T62) antibodies. (B) NCAP_SARS2 immunoprecipitation-PRM assays were developed with anti-NCAP_SARS2 mouse monoclonal MmAb (MM05), rabbit monoclonal RmAb (R001) and RmAb (R019), and rabbit polyclonal RpAb (T62) antibodies.

columns (2 cm × 100 μm, 5 μm C18) and separated on analytical columns (15 cm × 75 μm, 3 μm C18) using acetonitrile−water gradients at 400 nL/min.

Rapid IP-HPLC-SRM Assays. Following IP, addition of standards, and digestion on the same plate, digests were transferred onto HPLC autosampler-compatible 96-well microplates, and 17 μL of each digest was directly injected at 300 μL/min onto a trap column (30 mm × 2 mm; 3 μm C18). Peptides were separated on an analytical column (100 mm × 2 mm, 3 μm C18) using acetonitrile−water gradients at 100 μL/min. High-performance LC (Waters Acquity), Ion Drive Turbo V source, and QTRAP 6500+ (SCIEX) ensured sensitive and fast (12 min per injection) quantification of immunoglobulins. SRM parameters are presented in Table S7 in the Supporting Information. Each patient sample was measured with two analytical ("full process") replicates and three technical replicates. IgG and IgA were considered as monomers (2 copies of internal standard peptides per IgG or IgA), while IgM were pentamers (10 peptide copies per IgM).

ELISA. Time-resolved fluorescence (TRF) and colorimetric immunoassays were developed as previously described.[15,16] Briefly, S-ECD and N proteins spiked into serum were captured by primary antibodies (300 ng/well) and detected by in-house biotinylated secondary antibodies (40 ng/well). Alkaline phosphatase-conjugated streptavidin (1 μg/mL), 10 mM diflunisal phosphate, and 2 mM $TbCl_3$ enabled sensitive TRF detection through Tb-diflunisal-ethylenediamine tetraacetic acid (EDTA) complexes (excitation/emission 370/625 nm). To measure immunoglobulins, microplates were coated with S-ECD, S1, RBD, and N proteins (300 ng/well), blocked with 6% BSA, and incubated with 15,000-fold diluted patient sera. Secondary goat-anti-human IgG Fcγ (Invitrogen A18817) and goat-anti-human IgG/IgM/IgA H + L (Invitrogen A18847) were conjugated to HRP, which oxidized tetramethylbenzidine substrate for its detection at 450 nm.

RESULTS

Development of IP-SRM and IP-PRM Assays for the Quantification of SARS-CoV-2 Proteins. We obtained recombinant SARS-CoV-2 proteins, identified tryptic peptides by shotgun LC-MS/MS,[14] prioritized proteotypic peptides with the MaxQuant label-free quantification, and selected the most intense transitions. We also re-searched several public proteomic datasets[17,18] to confirm the choice of proteotypic peptides and determine relative abundances of SARS-CoV-2 proteins using label-free quantification: NCAP_SARS2 (55% of the viral proteome), VME1_SARS2 (18%), AP3A_SARS2 (9%), SPIKE_SARS2 (8%), ORF9B_SARS2 (7%), NS7A_SARS2 (1.2%), NS6_SARS2 (0.7%), NS8_SARS2 (0.4%), and others (~0.4%). A combined dataset of tryptic peptides and fragmentation spectra facilitated the selection of the best proteotypic peptides, which were synthesized and used as isotope-labeled standards for assay development. The selection of AYNVTQAFGR (NCAP_SARS2) and FLPFQQFGR (SPIKE_SARS2) as proteotypic peptides confirmed previous studies.[19] Following that, we developed SRM assays for

https://doi.org/10.1021/acs.analchem.2c01325
Anal. Chem. 2022, 94, 12990−12999

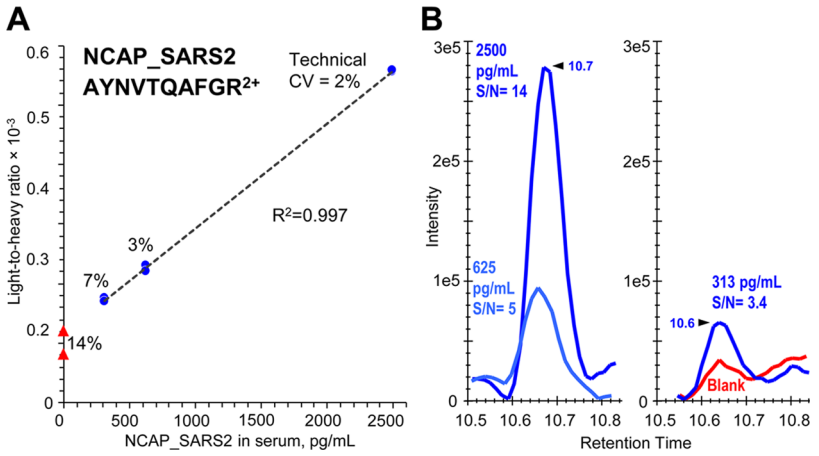

Figure 3. Quantification of recombinant NCAP_SARS2 protein spiked into human serum. Immunoprecipitation-PRM assay with RpAb T62 antibody revealed a linear response (A) and LOD of 313 pg/mL in serum (S/N > 3) or 170 amol on column (B). Red triangles and blue circles present blank measurements and concentrations above LOD, respectively.

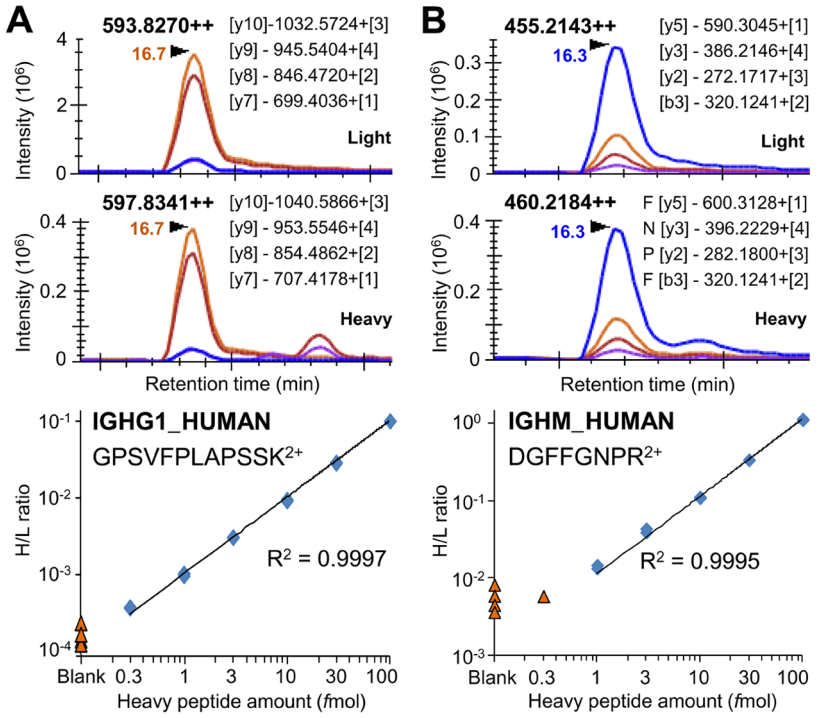

Figure 4. Representative SRM assays for quantification of IgG1 and IgM. Unique tryptic peptides located within CH1 domain of IGHG1_HUMAN and CH2 domain of IGHM_HUMAN were used as a proxy to quantify human IgG1 (A) and IgM (B), respectively. Calibration curves represented dilution series of heavy isotope-labeled peptide internal standards spiked into serum digest and revealed LOD 0.3 and 1 fmol on column to quantify IgG1 and IgM, respectively. Blue diamonds present amounts equal to or above LOD, while orange triangles present blank measurements or amounts below LOD.

quadrupole ion trap and PRM assays for quadrupole-Orbitrap mass spectrometers (Table S5). In our experience, PRM and SRM had comparable performance and could be readily transferred between these MS instruments.[20] To develop IP assays, we tested several anti-NCAP_SARS2 and anti-SPIKE_SARS2 antibodies and evaluated assay performance with the recombinant proteins spiked into human serum (Figures 2 and S2). As a result, the combined IP-PRM assay detected 1.25 ng/mL S-ECD of SPIKE_SARS2 (238 amol on column) and 313 pg/mL NCAP_SARS2 (170 amol on column) in serum (Figure 3). Comparable sensitivity was observed with our IP-SRM assay (Figure S3). It should be noted that the median levels of NCAP_SARS2 protein in capillary blood of symptomatic patients were recently reported as 1931 pg/mL,[21] well above the demonstrated limit of detections (LODs).

Quantification of Viral Proteins in Serum by In-House ELISA. To develop an in-house ELISA, we evaluated combinations of several anti-SPIKE_SARS2 and anti-NCAP_SARS2 antibodies for their efficiency to capture and detect their targets (Figure S4). Antibody pairs that provided the highest signal for the recombinant proteins in serum included: (i) a capture monoclonal CmAb D001 and a detection polyclonal RpAb T62 antibodies to measure S-ECD of SPIKE_SARS2 with LOQ of ~31 pg/mL (0.23 pM; 32 amol/well), and (ii) a capture polyclonal RpAb T62 and

https://doi.org/10.1021/acs.analchem.2c01325
Anal. Chem. 2022, 94, 12990−12999

detection monoclonal MmAb MM05 antibodies to measure NCAP_SARS2 with LOQ of ~15 pg/mL (0.32 pM; 23 amol/well) (Figure S5). For comparison, our TRF-ELISA revealed comparable or higher sensitivity relative to some commercial immunoassays (Sino Biological S1 0.8 pM and NCAP_SARS2 0.7 pM).

Development of IP-SRM Assays for Quantification of Anti-SARS-CoV-2 Immunoglobulins. Our approach for the differential quantification of immunoglobulin isotypes (IgG, IgM, IgA) and subclasses (IgG1-4, IgA1-2) relied on measurements of unique proteotypic peptides within the constant heavy chains (Figure S1). To select unique proteotypic peptides for each isotype and subclass, we searched Peptide Atlas, our previous proteomic datasets,[22] and literature data.[23,24] Selected proteotypic peptides represented all immunoglobulin allotypes.[25] GnomAD confirmed the lack of high-frequency missense variants (Table S4). Potential glycosylation sites or additional post-translational modifications were excluded using NextProt. Finally, synthetic heavy isotope-labeled peptides were used for assay development (Table S6). SRM assays for the quantification of IGHG1 and IGHM in direct digest of serum revealed LOQs of 0.3 and 1 fmol on column, respectively (Figure 4 and Table S8).

Selection of Antigen−Antibody Combinations with the Highest Diagnostic Performance. We evaluated numerous antigen−immunoglobulin isotype and subclass combinations by IP-SRM (Figure 5A) and by in-house indirect ELISA (Figures 5B and S6). Simultaneous evaluation of 36 combinations revealed 10 combinations with (i) statistically significant difference (MWU P-value < 0.05) and (ii) no overlap between groups suggesting high diagnostic performance; (Table S9). Ranking of combinations by the ratio of medians facilitated the selection of pairs with the highest dynamic range, such as RBD-IgG1 and S1-IgG1. Indirect ELISA confirmed RBD-IgG and S1-IgG as top combinations (Figure 5B) and was in agreement with previous studies.[26] Interestingly, S-ECD antigen revealed poor performance due to the high background in negative samples (Figure S7).

In addition to the rapid evaluation of numerous combinations, IP-SRM assays provided a nearly 2-fold wider dynamic range in comparison to indirect ELISA. The dynamic range of common affinity assays, including immunoassays, often does not exceed 3 orders of magnitude[27] and could be further limited by high background (nonspecific adsorption), lower signal (incomplete binding of secondary antibodies), signal saturation (excessive enzymatic reaction), and other factors. The direct quantification of immunoglobulin heavy chains by SRM simplified assay setup and eliminated background arising from nonspecific adsorption and cross-reactivity of secondary antibodies, thus increasing the overall dynamic range. The wider dynamic range of IP-SRM assays may facilitate earlier detection of seroconversion.

Quantification of Total and Anti-RBD Immunoglobulins by IP-SRM. Total immunoglobulin isotypes and subclasses were measured by SRM in direct digests of serum (median 2.8 mg/mL for IgG1 and 0.24 mg/mL for IgM) and agreed with the previously reported ranges (2.8−8.2 mg/mL for IgG1 and 0.2−2.3 mg/mL for IgM).[28,29] Anti-RBD IgG1, IgG3, IgM, and IgA1 subclasses, but not IgG2, IgG4, and IgA2, were found elevated in convalescent sera (Figure S8 and Table S10). Anti-RBD IgG1 were elevated in convalescent (510−6700 ng/mL; 0.02−0.22% of total serum IgG1) vs negative sera (60 [IQR 41−81] ng/mL). Anti-RBD IgG1 levels

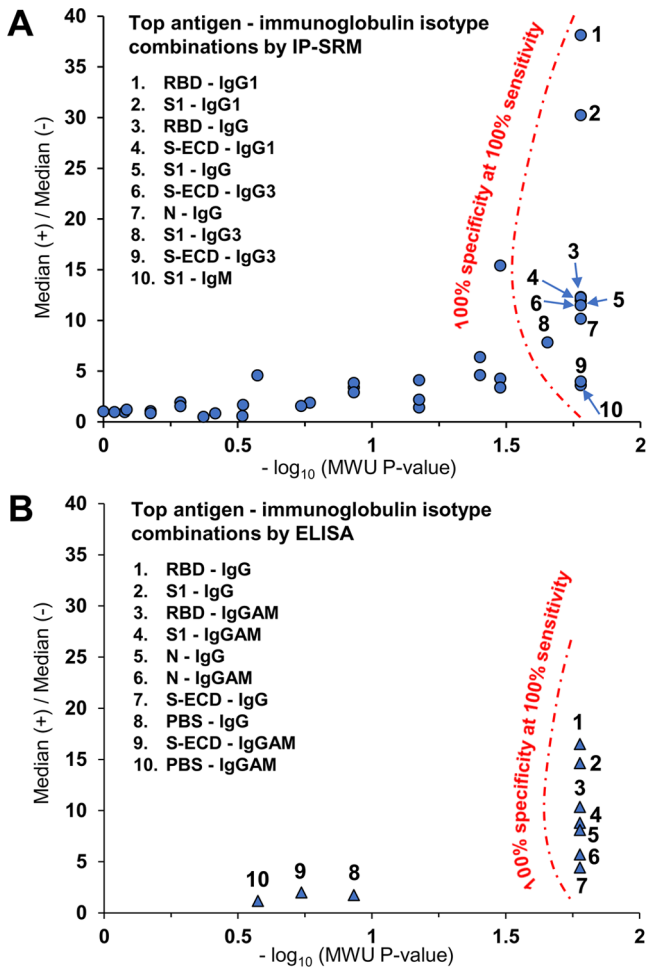

Figure 5. Rational design of SARS-CoV-2 serological tests. Roadmap for the evaluation of numerous antigen−immunoglobulin subclass combinations and selection of pairs with 100% diagnostic specificity and sensitivity based on IP-SRM (A) and indirect ELISA for IgG and IgG/A/M (B). Ranking of combinations by the ratio of medians facilitated the selection of pairs with the highest signal-to-noise ratio and dynamic range, such as RBD-IgG1 and S1-IgG1.

measured by IP-SRM well correlated (R^2 = 0.98) with IgG levels independently measured by SARS-CoV-2 IgG seroconversion ELISA (Table S10).

Absolute Quantification of Anti-RBD Immunoglobulin Isotypes and Subclasses and Validation of Their Diagnostic Performance with a Rapid Multiplex IP-HPLC-SRM Assay. To facilitate the analysis of 48 patient samples and >300 technical replicates (Table S11 and Figure 6), we further optimized sample preparation and developed a rapid multiplex IP-HPLC-SRM assay. Major advances included direct injection of digests and preconcentration of peptides onto trap columns, rapid peptide separations at 100 μL/min, fast and sensitive SRM acquisition with QTRAP 6500+, and semiautomated data analysis with Skyline. Heavy isotope-labeled peptides with trypsin-cleavable tags provided "absolute" quantification (ng/mL). Each sample was measured with two analytical replicates (IgG1 median analytical CV of 3% for positive and 15% for negative samples) and three technical replicates (IgG1 median technical CV of 1.6% for positive and 1.7% for negative samples). No significant differences were found for serum versus EDTA plasma (IgG1 MWU P = 0.46). A high correlation was found for peptides representing total

https://doi.org/10.1021/acs.analchem.2c01325
Anal. Chem. 2022, 94, 12990−12999

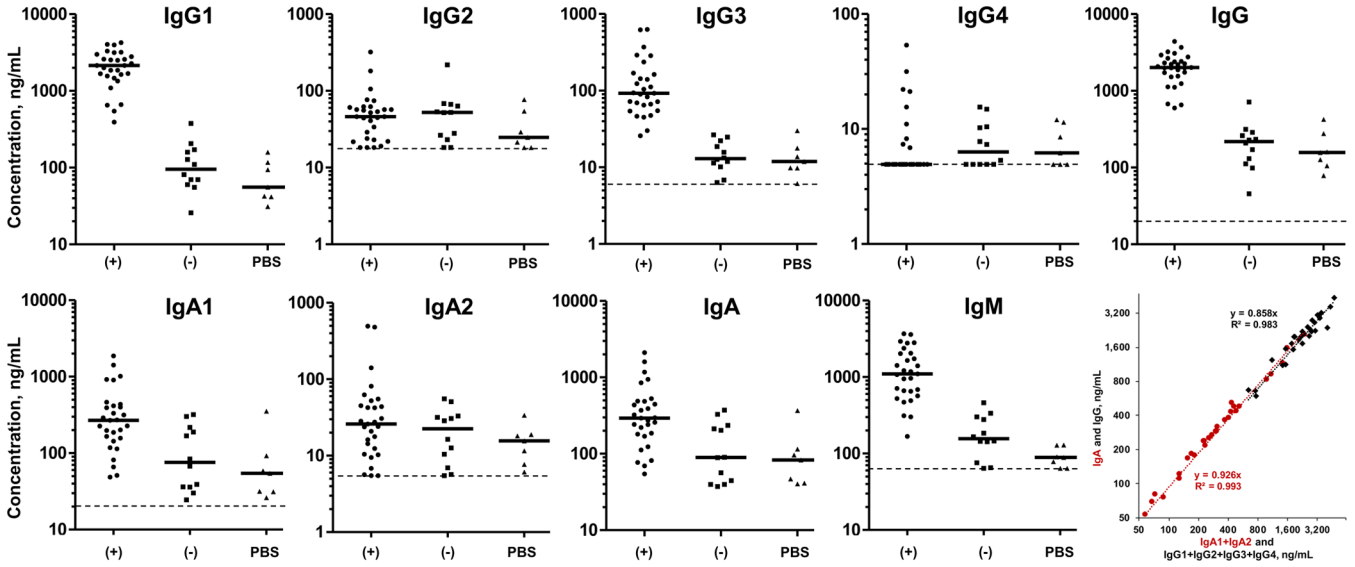

Figure 6. Absolute quantification of anti-RBD immunoglobulin subclasses and validation of their diagnostic performance using the rapid IP-HPLC-SRM assay. Simple 96-well microplate IP setup, direct injection of digests, rapid extraction of peptides with a trap column at 300 μL/min, and rapid peptide separations (100 μL/min; 12 min per injection) provided high reproducibility (3% analytical CV) and throughput of 120 technical replicates/day. Positive samples (+), N = 29, included EDTA plasma of PCR-confirmed patients. Negative samples (−) included sera collected before 11−2019 (N = 7) and EDTA plasma of PCR-confirmed patients (N = 5). Controls included PBS-coated plates with positive EDTA plasma (N = 4) and negative serum (N = 3). Each sample was measured with two analytical (independent IP) and three technical replicates. Dashed lines represent peptide LODs (signal-to-noise ratio > 3 within the linear response range), and the values below LOD were adjusted to the LOD levels. A high correlation was found for peptides representing the total isotype levels versus the sum of individual subclasses (IgG vs IgG1 + IgG2 + IgG3 + IgG4, and IgA vs IgA1 + IgA2, respectively).

Table 1. Validation of the Diagnostic Performance of Anti-RBD Immunoglobulin Isotypes and Subclasses, as Measured by Multiplex IP-HPLC-SRM[a]

subclass	(+) median concentration (ng/mL)	(−) median concentration (ng/mL)	ratio (+)/(−)	1-tail MWU P-value	AUC	cutoff (ng/mL)	specificity at 100% sensitivity, % [95% CI]	phosphate-buffered saline (PBS) control, median ng/mL
IgG1	2138	95	22	3.3×10^{-7}	1.00 [1.00−1.00]	385	100 [74−100]	56
IgG3	92	13	7.1	3.9×10^{-7}	0.997 [0.99−1.00]	25	92 [62−100]	12
IgG (total)	2017	218	9.2	5.2×10^{-7}	0.99 [0.97−1.01]	457	92 [62−100]	157
IgM	1100	156	7.1	1.4×10^{-6}	0.97 [0.93−1.01]	166	58 [28−85]	89
IgA1	269	76	3.6	2.0×10^{-3}	0.79 [0.64−0.94]	44	42 [15−72]	54
IgA (total)	293	90	3.3	1.8×10^{-3}	0.79 [0.65−0.94]	50	33 [10−65]	83
IgA2	26	22	1.2	0.24	0.57 [0.38−0.76]			16
IgG2	46	52	0.9	0.51	0.50 [0.30−0.70]			25
IgG4	4.9	6.3	0.8	0.87	0.60 [0.41−0.79]			6.2

[a]Samples included positive (+) convalescent plasma (N = 29) and negative (−) plasma (N = 5) and serum (N = 7); PBS controls included positive plasma (N = 4) and negative serum (N = 3).

IgG or IgA, and the sum of individual subclasses (IgG1-4 or IgA1-2, respectively; Figure 6). As a result, anti-RBD IgG1, IgG3, IgM, and IgA1 levels were elevated 22-, 7-, 7-, and 3.6-fold in positive COVID-19-convalescent plasma, respectively, while IgG2, IgG4, and IgA2 levels were not informative (Table 1). Anti-RBD IgG1 levels in positive (median 2138 [IQR 1565−2794] ng/mL) vs negative samples (95 [IQR 67−162] ng/mL) revealed a diagnostic cutoff of 385 ng/mL, which provided 100% diagnostic specificity and sensitivity to detect COVID-19-convalescent plasma. Interestingly, IgE and IgD isotypes (the least abundant plasma immunoglobulins potentially not involved in SARS-CoV-2 immune response) were not detected in any convalescent any plasma, serum, or saliva samples. While anti-RBD IgG2, IgG4, and IgA2 levels were generally low, some convalescent plasma revealed high levels of IgG2 (321 ng/mL), IgG4 (54 ng/mL), and IgA2 (495 ng/mL). In future, this phenomenon could be investigated in more detail.

Measurement of Anti-RBD Immunoglobulins in Saliva. To assess the potential for noninvasive diagnostics, we measured anti-RBD immunoglobulins by IP-HPLC-SRM in 25 convalescent saliva (Figure 7). Since saliva of prepandemic or unvaccinated individuals was unavailable, nonspecific binding was estimated with convalescent saliva and PBS instead of RBD. Interestingly, IgA1 (monomer equivalents) were the most abundant isotype in convalescent saliva. The median levels of IgA1, IgG1, and IgM were 7-, 150-, and 190-fold lower, respectively, in saliva compared to plasma (Table 1). Other isotypes and subclasses were undetectable in saliva.

https://doi.org/10.1021/acs.analchem.2c01325
Anal. Chem. 2022, 94, 12990−12999

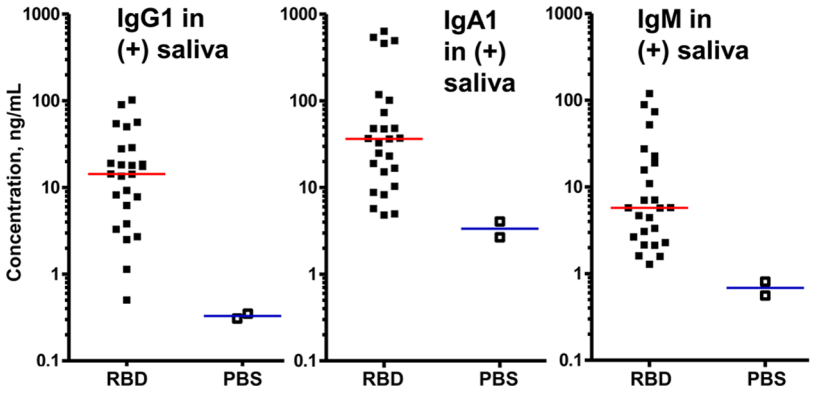

Figure 7. Quantification of anti-RBD IgG1, IgA1, and IgM in saliva of COVID-19 convalescent patients. IgA1 was the most abundant isotype in convalescent saliva (N = 25). Nonspecific binding was estimated with convalescent saliva samples and PBS instead of RBD antigen.

DISCUSSION

Infectious disease diagnostics has been revolutionized with the advent of PCR and RT-PCR. Routine diagnostics is now increasingly utilizing protein and immunoglobulin measurements to aid nucleic acids tests and provide additional diagnostic information. Hepatitis B testing is a prominent example and includes PCR measurements of viral DNA and immunoassay measurements of viral proteins and corresponding IgG and IgM. Different combinations of positive and negative outcomes provide a detailed interpretation of Hepatitis B status (acute, chronic, etc.).[5] It should be noted that the lower analytical sensitivity of protein assays, compared to PCR, could be leveraged by the presence of numerous protein copies (~1000 copies of NCAP_SARS2 per virion[30]), high serum antibody titters (2 μg/mL or 10^{13} copies/mL of anti-RBD IgG1), longer elimination half-life for circulating viral proteins vs RNA,[31] and higher preanalytical stability of proteins.

The design of conventional serological tests has not changed for decades and utilized conservative immunoassay approaches, with a focus on convenience, speed of manufacturing, and affordability. Limitations of such tests included semiquantitative measurements, lack of reference standards, potential cross-reactivity, and no differentiation between human immunoglobulin subclasses. Lack of international reference standards for serological assay calibration at the early stages of COVID-19 pandemic (each hospital utilized convalescent sera of their patients) limited interlaboratory standardization of serological tests. As a result of cross-reactivity, diagnostic specificity of serological antibody tests was not sufficiently high to enable screening of asymptomatic population for the acquired immunity against low-prevalence infectious diseases, such as COVID-19. A serological test with a 90% PPV during the early stages of pandemic (~0.1% disease prevalence) would require 99.99% diagnostic specificity, while the median diagnostic specificity of ~60 FDA-authorized serological tests is currently 99.3%[7] and allows for testing populations with >6% COVID-19 prevalence. These limitations need to be addressed with the new generation of serological tests.

MS has previously been used for the identification and quantification of the SARS-CoV-2 proteins in clinical samples.[9−11] Since systematic discovery and development of protein biomarkers involves numerous stages of verification and validation, MS assays due to their rapid design and execution are particularly useful at the early stages of biomarker discovery and development of diagnostic assays.[32−35] Without extensive fractionation, however, MS assays present relatively poor analytical sensitivity. Here, we suggested that a combination of immunoaffinity enrichment with MS measurements would provide sensitive and selective serological assays to measure viral proteins and antiviral immunoglobulins. The proposed IP-SRM/PRM assays combine the advantages of two worlds: immunoassays with their high analytical sensitivity and SRM/PRM with high analytical selectivity.[36−39] We previously demonstrated that SRM and PRM assays provided robust tools for the quantification of proteins in human cell lines,[40,41] primary cells,[42,43] tissues,[16] biological fluids,[44−50] and serum.[51] Additional IP resulted in a 1000-fold increase in sensitivity, reaching sub-ng/mL (<10 pM) levels for IP-SRM in biological samples.[20] In this study, IP-PRM and IP-SRM assays detected as little as 313 and 500 pg/mL NCAP_SARS2, respectively, well below the previously reported NCAP_SARS2 levels in serum symptomatic patients (1931 pg/mL).[21]

In addition, our multiplex IP-SRM assay facilitated simultaneous evaluation of numerous antigen−immunoglobulin subclass combinations and revealed RBD-IgG1 as a combination with the highest diagnostic specificity and sensitivity. Our diagnostic cutoffs (0.39 for IgG1 and 0.46 μg/mL for total IgG) were comparable to the cutoffs of conventional SARS-CoV-2 IgG serological tests (0.77 μg/mL for total IgG[52]). Elevated levels of anti-RBD total IgG, total IgA, IgG1, IgG3, IgM, and IgA1, but not IgG2, IgG4, IgA2, IgD, or IgE, were identified. A combined IP-SRM assay (Tables S5 and S6) could enable measurements of SARS-CoV-2 antigens and immunoglobulins with a single platform.

Furthermore, measurements of anti-SARS-CoV-2 immunoglobulins in saliva suggested the feasibility of noninvasive diagnostics. It should be noted that while salivary IgG are derived from serum by passive diffusion, salivary IgA are mainly produced locally by plasma cells in salivary glands and secreted into saliva as J chain- and secretory component-containing dimeric IgA. As a result, the serum and salivary IgA pools have different structures and concentrations. Assuming similar rates of diffusion for IgG1 and monomeric IgA1 from serum, our data (Table 1 and Figure 7) suggested that ~95% of salivary IgA1 (monomer equivalents) could be produced locally.

While analysis of the complete set of human immunoglobulin isotypes and subclasses could not be justified for the routine measurements by indirect ELISA (11 independent assays and 11 measurements per sample would be required),

https://doi.org/10.1021/acs.analchem.2c01325
Anal. Chem. 2022, 94, 12990−12999

the complete set could provide additional diagnostic and prognostic information. Indeed, the subclass identity and circulating levels of immunoglobulins vary during the course of infection and depend on the dynamics of class switching, time after exposure, antigen identity (peptides or polysaccharides), route of infection (respiratory or topical), cell-mediated immunity (type 1 or 2 helper T cells), subclass stability (shorter half-life IgG3), affinity, and effector functions (cytotoxicity or phagocytosis).[25]

Finally, the following limitations of our study should be discussed: (i) a relatively low sample size to enable accurate estimations of diagnostic performance and cutoffs; (ii) relatively low throughput of IP-HPLC-SRM to enable high-volume testing; (iii) detailed evaluation of immunoglobulins produced against RBD but no other antigens; (iv) recognized limitations of antibody-based assays, such as requirement for high-quality antibodies for IP. While IP-HPLC-MS cannot provide the throughput required for population-based studies (thousands of samples per day), our assays could be novel tools to complement indirect immunoassays in serological studies, clinical research, and small-scale preclinical studies (up to 120 samples per day). Rational design of serological assays, independent validation of cross-reactivity, multiplexing, absolute quantification (μg/mL vs dilution factors or antibody titers[53]), and stable and affordable reference standards are the advantages of IP-SRM serological assays. It should be mentioned that clinical-grade IP-LC-SRM assays are being actively introduced into clinical laboratories.[54]

In future, IP-LC-SRM assays may have a potential for application in clinical laboratories, provided the following limitations are addressed: (i) improvement of assay throughput; (ii) training of highly qualified personnel; (iii) reducing costs of immunoprecipitation-mass spectrometry (IP-MS) assays through automation; (iv) evaluation of diagnostic specificity with the larger sample sets (such as >143 negative samples to evaluate diagnostic specificity higher than the specificity of the conventional SARS-CoV-2 serological tests of 99.3%); (v) more sensitive and antibody-free measurements of protein antigens using the next-generation MS instruments and advances in ion mobility, alternative peptide fragmentation modes, and improved ion transmission efficiency. Relatively low throughput of IP-HPLC-MS assays, an apparent limitation for their clinical implementation, could be improved through: (i) automation of IP and proteomic sample preparation; (ii) faster separations using shorter LC columns and sub-2 μm particles; (iii) multichannel and turbulent flow LC with intelligent scheduling to enable parallel online cleanup and analysis;[10] and (iv) LC-independent paper spray SRM analysis of dried blood spots.[55]

CONCLUSIONS

We conclude that immunoprecipitation-targeted proteomic assays may improve the design and facilitate the development of serological tests, provide assay standardization, and enable independent evaluation of conventional serological immunoassays. Increased diagnostic specificity of the improved serological tests would enable evidence-based screening of broader populations for the acquired immunity. IP-SRM assays targeting novel antigens or mutated epitopes could be developed within weeks and enable functional and translational studies of emerging pathogens. Future developments of IP-MS for analysis of human immunoglobulins may facilitate the selection of affinity binders and antibodies with desired affinity[56−58] and subclass identity, and eventually evolve into approaches for sequencing of the clinically useful immunoglobulins directly from the patient's blood, thus paving the way for rapid development of next-generation therapeutic antibodies.

ASSOCIATED CONTENT

Supporting Information

The Supporting Information is available free of charge at https://pubs.acs.org/doi/10.1021/acs.analchem.2c01325.

Experimental protocols; supporting figures; and STARD2015 recommendations (PDF)

Patient samples, antibodies, and recombinant proteins; and SRM and PRM assay parameters (XLSX)

AUTHOR INFORMATION

Corresponding Author

Andrei P. Drabovich − *Division of Analytical and Environmental Toxicology, Department of Laboratory Medicine and Pathology, Faculty of Medicine and Dentistry, University of Alberta, Edmonton, Alberta T6G 2R3, Canada;* orcid.org/0000-0003-3049-7145; Phone: 780-492-1190; Email: andrei.drabovich@ualberta.ca

Authors

Zhiqiang Fu − *Division of Analytical and Environmental Toxicology, Department of Laboratory Medicine and Pathology, Faculty of Medicine and Dentistry, University of Alberta, Edmonton, Alberta T6G 2R3, Canada*

Yasmine Rais − *Division of Analytical and Environmental Toxicology, Department of Laboratory Medicine and Pathology, Faculty of Medicine and Dentistry, University of Alberta, Edmonton, Alberta T6G 2R3, Canada*

Delaram Dara − *Division of Analytical and Environmental Toxicology, Department of Laboratory Medicine and Pathology, Faculty of Medicine and Dentistry, University of Alberta, Edmonton, Alberta T6G 2R3, Canada*

Dana Jackson − *Department of Medicine, Faculty of Medicine and Dentistry, University of Alberta, Edmonton, Alberta T6G 2R3, Canada*

Complete contact information is available at: https://pubs.acs.org/10.1021/acs.analchem.2c01325

Author Contributions

[§]Z.F. and Y.R. contributed equally. A.P.D. conceived the study. Z.F. and Y.R. performed experiments. A.P.D., Z.F., and Y.R. analyzed data. D.J. documented patient data and retrieved clinical samples. A.P.D., Z.F., and Y.R. wrote the manuscript, and all authors contributed to revisions.

Notes

The authors declare no competing financial interest.

ACKNOWLEDGMENTS

The authors thank Dr. Xingfang Li for the access to QTRAP 5500, and Canadian BioSample Repository and Dr. Bruce Ritchie for access to clinical samples. This work was supported by the Canadian Institutes of Health Research COVID-19 Immunity Task Force grant (#VR2-173207) and Alberta Innovates National Partnered R&I Initiatives (#202100452) to A.P.D. Z.F. acknowledges the National Natural Science Foundation of China (21806018) and Globalink Early Career Fellowship (Mitacs, China Scholarship Council; 201806065018).

NONSTANDARD ABBREVIATIONS

AUC	area under the receiver operating characteristic curve
CV	coefficient of variation
IQR	interquartile range
LC-MS/MS	liquid chromatography-tandem mass spectrometry
L/H	light-to-heavy ratio
LOD	limit of detection
LOQ	limit of quantification
mAb	monoclonal antibody
MWU	Mann−Whitney U test
OD	optical density
PBS	phosphate-buffered saline
PRM	parallel reaction monitoring
SRM	selected reaction monitoring
TRF	time-resolved fluorescence

REFERENCES

(1) Feng, W.; Newbigging, A. M.; Le, C.; Pang, B.; Peng, H.; Cao, Y.; Wu, J.; Abbas, G.; Song, J.; Wang, D. B.; Cui, M.; Tao, J.; Tyrrell, D. L.; Zhang, X. E.; Zhang, H.; Le, X. C. *Anal. Chem.* **2020**, *92*, 10196−10209.

(2) Kanji, J. N.; Zelyas, N.; MacDonald, C.; Pabbaraju, K.; Khan, M. N.; Prasad, A.; Hu, J.; Diggle, M.; Berenger, B. M.; Tipples, G. *Virol. J.* **2021**, *18*, No. 13.

(3) Rais, Y.; Fu, Z.; Drabovich, A. P. *Clin. Proteomics* **2021**, *18*, No. 19.

(4) Liu, G.; Rusling, J. F. *ACS Sens.* **2021**, *6*, 593−612.

(5) Hwang, J. P.; Feld, J. J.; Hammond, S. P.; Wang, S. H.; Alston-Johnson, D. E.; Cryer, D. R.; Hershman, D. L.; Loehrer, A. P.; Sabichi, A. L.; Symington, B. E.; Terrault, N.; Wong, M. L.; Somerfield, M. R.; Artz, A. S. *J. Clin. Oncol.* **2020**, *38*, 3698−3715.

(6) Isho, B.; Abe, K. T.; Zuo, M.; Jamal, A. J.; Rathod, B.; Wang, J. H.; Li, Z.; Chao, G.; Rojas, O. L.; Bang, Y. M.; Pu, A.; Christie-Holmes, N.; Gervais, C.; Ceccarelli, D.; Samavarchi-Tehrani, P.; Guvenc, F.; Budylowski, P.; Li, A.; Paterson, A.; Yue, F. Y.; Marin, L. M.; Caldwell, L.; Wrana, J. L.; Colwill, K.; Sicheri, F.; Mubareka, S.; Gray-Owen, S. D.; Drews, S. J.; Siqueira, W. L.; Barrios-Rodiles, M.; Ostrowski, M.; Rini, J. M.; Durocher, Y.; McGeer, A. J.; Gommerman, J. L.; Gingras, A. C. *Sci. Immunol.* **2020**, *5*, No. eabe5511.

(7) Brownstein, N. C.; Chen, Y. A. *Sci. Rep.* **2021**, *11*, No. 5491.

(8) Wee, S.; Alli-Shaik, A.; Kek, R.; Swa, H. L. F.; Tien, W. P.; Lim, V. W.; Leo, Y. S.; Ng, L. C.; Hapuarachchi, H. C.; Gunaratne, J. *Proc. Natl. Acad. Sci. U.S.A.* **2019**, *116*, 6754−6759.

(9) Zecha, J.; Lee, C. Y.; Bayer, F. P.; Meng, C.; Grass, V.; Zerweck, J.; Schnatbaum, K.; Michler, T.; Pichlmair, A.; Ludwig, C.; Kuster, B. *Mol. Cell. Proteomics* **2020**, *19*, 1503−1522.

(10) Cardozo, K. H. M.; Lebkuchen, A.; Okai, G. G.; Schuch, R. A.; Viana, L. G.; Olive, A. N.; Lazari, C. D. S.; Fraga, A. M.; Granato, C. F. H.; Pintao, M. C. T.; Carvalho, V. M. *Nat. Commun.* **2020**, *11*, No. 6201.

(11) Cazares, L. H.; Chaerkady, R.; Samuel Weng, S. H.; Boo, C. C.; Cimbro, R.; Hsu, H. E.; Rajan, S.; Dall'Acqua, W.; Clarke, L.; Ren, K.; McTamney, P.; Kallewaard-LeLay, N.; Ghaedi, M.; Ikeda, Y.; Hess, S. *Anal. Chem.* **2020**, *92*, 13813−13821.

(12) Ihling, C.; Tanzler, D.; Hagemann, S.; Kehlen, A.; Huttelmaier, S.; Arlt, C.; Sinz, A. *J. Proteome Res.* **2020**, *19*, 4389−4392.

(13) Renuse, S.; Vanderboom, P. M.; Maus, A. D.; Kemp, J. V.; Gurtner, K. M.; Madugundu, A. K.; Chavan, S.; Peterson, J. A.; Madden, B. J.; Mangalaparthi, K. K.; Mun, D. G.; Singh, S.; Kipp, B. R.; Dasari, S.; Singh, R. J.; Grebe, S. K.; Pandey, A. *EBioMedicine* **2021**, *69*, No. 103465.

(14) Fu, Z.; Drabovich, A. P.LC-MS/MS analysis of recombinant Spike and Nucleocapsid proteins [Data set] *Zenodo*, 2020 https://doi.org/10.5281/zenodo.3743880.

(15) Korbakis, D.; Schiza, C.; Brinc, D.; Soosaipillai, A.; Karakosta, T. D.; Legare, C.; Sullivan, R.; Mullen, B.; Jarvi, K.; Diamandis, E. P.; Drabovich, A. P. *BMC Med.* **2017**, *15*, No. 60.

(16) Fu, Z.; Rais, Y.; Bismar, T. A.; Hyndman, M. E.; Le, X. C.; Drabovich, A. P. *Mol. Cell. Proteomics* **2021**, *20*, No. 100075.

(17) Davidson, A. D.; Williamson, M. K.; Lewis, S.; Shoemark, D.; Carroll, M. W.; Heesom, K. J.; Zambon, M.; Ellis, J.; Lewis, P. A.; Hiscox, J. A.; Matthews, D. A. *Genome Med.* **2020**, *12*, No. 68.

(18) Bojkova, D.; Klann, K.; Koch, B.; Widera, M.; Krause, D.; Ciesek, S.; Cinatl, J.; Munch, C. *Nature* **2020**, *583*, 469−472.

(19) Grossegesse, M.; Hartkopf, F.; Nitsche, A.; Schaade, L.; Doellinger, J.; Muth, T. *J. Proteome Res.* **2020**, *19*, 4380−4388.

(20) Karakosta, T. D.; Soosaipillai, A.; Diamandis, E. P.; Batruch, I.; Drabovich, A. P. *Mol. Cell. Proteomics* **2016**, *15*, 2863−2876.

(21) Shan, D.; Johnson, J. M.; Fernandes, S. C.; Suib, H.; Hwang, S.; Wuelfing, D.; Mendes, M.; Holdridge, M.; Burke, E. M.; Beauregard, K.; Zhang, Y.; Cleary, M.; Xu, S.; Yao, X.; Patel, P. P.; Plavina, T.; Wilson, D. H.; Chang, L.; Kaiser, K. M.; Nattermann, J.; Schmidt, S. V.; Latz, E.; Hrusovsky, K.; Mattoon, D.; Ball, A. J. *Nat. Commun.* **2021**, *12*, No. 1931.

(22) Schiza, C.; Korbakis, D.; Jarvi, K.; Diamandis, E. P.; Drabovich, A. P. *Mol. Cell. Proteomics* **2019**, *18*, 338−351.

(23) Ladwig, P. M.; Barnidge, D. R.; Snyder, M. R.; Katzmann, J. A.; Murray, D. L. *Clin. Chem.* **2014**, *60*, 1080−1088.

(24) Remily-Wood, E. R.; Benson, K.; Baz, R. C.; Chen, Y. A.; Hussein, M.; Hartley-Brown, M. A.; Sprung, R. W.; Perez, B.; Liu, R. Z.; Yoder, S. J.; Teer, J. K.; Eschrich, S. A.; Koomen, J. M. *Proteomics Clin. Appl.* **2014**, *8*, 783−795.

(25) Vidarsson, G.; Dekkers, G.; Rispens, T. *Front Immunol* **2014**, *5*, No. 520.

(26) Premkumar, L.; Segovia-Chumbez, B.; Jadi, R.; Martinez, D. R.; Raut, R.; Markmann, A.; Cornaby, C.; Bartelt, L.; Weiss, S.; Park, Y.; Edwards, C. E.; Weimer, E.; Scherer, E. M.; Rouphael, N.; Edupuganti, S.; Weiskopf, D.; Tse, L. V.; Hou, Y. J.; Margolis, D.; Sette, A.; Collins, M. H.; Schmitz, J.; Baric, R. S.; de Silva, A. M. *Sci. Immunol.* **2020**, *5*, No. eabc8413.

(27) Drabovich, A. P.; Okhonin, V.; Berezovski, M.; Krylov, S. N. *J. Am. Chem. Soc.* **2007**, *129*, 7260−7261.

(28) French, M. A.; Harrison, G. *Clin. Exp. Immunol.* **1984**, *56*, 18−22.

(29) Puissant-Lubrano, B.; Peres, M.; Apoil, P. A.; Congy-Jolivet, N.; Roubinet, F.; Blancher, A. *Clin. Chem. Lab. Med.* **2015**, *53*, e359−e361.

(30) Bar-On, Y. M.; Flamholz, A.; Phillips, R.; Milo, R. *eLife* **2020**, *9*, No. e57309.

(31) Li, Y. H.; Li, J.; Liu, X. E.; Wang, L.; Li, T.; Zhou, Y. H.; Zhuang, H. *J. Virol. Methods* **2005**, *130*, 45−50.

(32) Drabovich, A. P.; Martinez-Morillo, E.; Diamandis, E. P. *Biochim. Biophys. Acta, Proteins Proteomics* **2015**, *1854*, 677−686.

(33) Drabovich, A. P.; Pavlou, M. P.; Batruch, I.; Diamandis, E. P. Proteomic and mass spectrometry technologies for biomarker discovery. In *Proteomic and Metabolomic Approaches to Biomarker Discovery*; Issaq, H. J.; Veenstra, T. D., Eds.; Academic Press (Elsevier): Waltham, MA, 2013; Chapter 2, pp 17−37.

(34) Drabovich, A. P.; Saraon, P.; Jarvi, K.; Diamandis, E. P. *Nat. Rev. Urol.* **2014**, *11*, 278−288.

(35) Drabovich, A. P.; Martínez-Morillo, E.; Diamandis, E. P. Protein Biomarker Discovery. In *Proteomics for Biological Discover*, 2nd ed.; Veenstra, T. D.; Yates, J. R., III, Eds.; John Wiley & Sons, 2019; Chapter 3, pp 63−88.

(36) Drabovich, A. P.; Dimitromanolakis, A.; Saraon, P.; Soosaipillai, A.; Batruch, I.; Mullen, B.; Jarvi, K.; Diamandis, E. P. *Sci. Transl. Med.* **2013**, *5*, No. 212ra160.

(37) Korbakis, D.; Brinc, D.; Schiza, C.; Soosaipillai, A.; Jarvi, K.; Drabovich, A. P.; Diamandis, E. P. *Mol. Cell. Proteomics* **2015**, *14*, 1517−1526.

(38) Drabovich, A. P.; Saraon, P.; Drabovich, M.; Karakosta, T. D.; Dimitromanolakis, A.; Hyndman, M. E.; Jarvi, K.; Diamandis, E. P. *Mol. Cell. Proteomics* **2019**, *18*, 1807−1823.

(39) Schiza, C.; Korbakis, D.; Panteleli, E.; Jarvi, K.; Drabovich, A. P.; Diamandis, E. P. *Mol. Cell. Proteomics* **2018**, *17*, 2480−2495.
(40) Drabovich, A. P.; Pavlou, M. P.; Dimitromanolakis, A.; Diamandis, E. P. *Mol. Cell. Proteomics* **2012**, *11*, 422−434.
(41) Drabovich, A. P.; Pavlou, M. P.; Schiza, C.; Diamandis, E. P. *Mol. Cell. Proteomics* **2016**, *15*, 2093−2107.
(42) Konvalinka, A.; Zhou, J.; Dimitromanolakis, A.; Drabovich, A. P.; Fang, F.; Gurley, S.; Coffman, T.; John, R.; Zhang, S. L.; Diamandis, E. P.; Scholey, J. W. *J. Biol. Chem.* **2013**, *288*, 24834−24847.
(43) Cho, C. K.; Drabovich, A. P.; Karagiannis, G. S.; Martinez-Morillo, E.; Dason, S.; Dimitromanolakis, A.; Diamandis, E. P. *Clin. Proteomics* **2013**, *10*, No. 2.
(44) Begcevic, I.; Brinc, D.; Drabovich, A. P.; Batruch, I.; Diamandis, E. P. *Clin. Proteomics* **2016**, *13*, No. 11.
(45) Begcevic, I.; Brinc, D.; Dukic, L.; Simundic, A. M.; Zavoreo, I.; Basic Kes, V.; Martinez-Morillo, E.; Batruch, I.; Drabovich, A. P.; Diamandis, E. P. *J. Proteome Res.* **2018**, *17*, 2282−2292.
(46) Martínez-Morillo, E.; Cho, C. K.; Drabovich, A. P.; Shaw, J. L.; Soosaipillai, A.; Diamandis, E. P. *J. Proteome Res.* **2012**, *11*, 3880−3887.
(47) Martínez-Morillo, E.; Nielsen, H. M.; Batruch, I.; Drabovich, A. P.; Begcevic, I.; Lopez, M. F.; Minthon, L.; Bu, G.; Mattsson, N.; Portelius, E.; Hansson, O.; Diamandis, E. P. *J. Proteome Res.* **2014**, *13*, 1077−1087.
(48) Drabovich, A. P.; Jarvi, K.; Diamandis, E. P. *Mol. Cell. Proteomics* **2011**, *10*, No. M110.004127.
(49) Cho, C. K.; Drabovich, A. P.; Batruch, I.; Diamandis, E. P. *J. Proteomics* **2011**, *74*, 2052−2059.
(50) Konvalinka, A.; Batruch, I.; Tokar, T.; Dimitromanolakis, A.; Reid, S.; Song, X.; Pei, Y.; Drabovich, A. P.; Diamandis, E. P.; Jurisica, I.; Scholey, J. W. *Clin. Proteomics* **2016**, *13*, No. 16.
(51) Drabovich, A. P.; Diamandis, E. P. *J. Proteome Res.* **2010**, *9*, 1236−1245.
(52) Norman, M.; Gilboa, T.; Ogata, A. F.; Maley, A. M.; Cohen, L.; Busch, E. L.; Lazarovits, R.; Mao, C. P.; Cai, Y.; Zhang, J.; Feldman, J. E.; Hauser, B. M.; Caradonna, T. M.; Chen, B.; Schmidt, A. G.; Alter, G.; Charles, R. C.; Ryan, E. T.; Walt, D. R. *Nat. Biomed. Eng.* **2020**, *4*, 1180−1187.
(53) Amanat, F.; Stadlbauer, D.; Strohmeier, S.; Nguyen, T. H. O.; Chromikova, V.; McMahon, M.; Jiang, K.; Arunkumar, G. A.; Jurczyszak, D.; Polanco, J.; Bermudez-Gonzalez, M.; Kleiner, G.; Aydillo, T.; Miorin, L.; Fierer, D. S.; Lugo, L. A.; Kojic, E. M.; Stoever, J.; Liu, S. T. H.; Cunningham-Rundles, C.; Felgner, P. L.; Moran, T.; Garcia-Sastre, A.; Caplivski, D.; Cheng, A. C.; Kedzierska, K.; Vapalahti, O.; Hepojoki, J. M.; Simon, V.; Krammer, F. *Nat. Med.* **2020**, *26*, 1033−1036.
(54) Netzel, B. C.; Grant, R. P.; Hoofnagle, A. N.; Rockwood, A. L.; Shuford, C. M.; Grebe, S. K. *Clin. Chem.* **2016**, *62*, 297−299.
(55) Yannell, K. E.; Kesely, K. R.; Chien, H. D.; Kissinger, C. B.; Cooks, R. G. *Anal. Bioanal. Chem.* **2017**, *409*, 121−131.
(56) Drabovich, A.; Berezovski, M.; Krylov, S. N. *J. Am. Chem. Soc.* **2005**, *127*, 11224−11225.
(57) Drabovich, A. P.; Berezovski, M.; Okhonin, V.; Krylov, S. N. *Anal. Chem.* **2006**, *78*, 3171−3178.
(58) Drabovich, A. P.; Berezovski, M. V.; Musheev, M. U.; Krylov, S. N. *Anal. Chem.* **2009**, *81*, 490−494.

https://doi.org/10.1021/acs.analchem.2c01325
Anal. Chem. 2022, 94, 12990−12999